

Nonlinear three-magnon scattering in low-damping $La_{0.67}Sr_{0.33}MnO_3$ thin films

Yuelin Zhang(张跃林), Lutong Sheng(盛路通) Jilei Chen(陈济雷), Jie Wang(王婕), Zengtai Zhu(朱增泰), Rundong Yuan(袁润东) Jingdi Lu(鲁京迪), Hanchen Wang(王涵晨) Sijie Hao(郝思洁), Peng Chen(陈鹏), Guoqiang Yu(于国强), Xiufeng Han(韩秀峰), and Haiming Yu(于海明)
Citation: Chin. Phys. B, 2023, 32 (**10**): 107505. DOI: 10.1088/1674-1056/acedf8
Journal homepage: http://cpb.iphy.ac.cn; http://iopscience.iop.org/cpb

What follows is a list of articles you may be interested in

Asymmetric scattering behaviors of spin wave dependenton magnetic vortex chirality

Xue-Feng Zhang(张雪枫), Je-Ho Shim(沈帝虎), Xiao-Ping Ma(马晓萍), Cheng Song(宋成), Haiming Yu(于海明), and Hong-Guang Piao(朴红光)
Chin. Phys. B, 2023, 32 (**10**): 107501. DOI: 10.1088/1674-1056/acd36a

Angle-dependent spin wave spectra of permalloy ring arrays

Shuxuan Wu(吴书旋), Zengtai Zhu(朱增泰), Yunxu Ma(马云旭), Jinwu Wei(魏晋武), Senfu Zhang(张森富), Jianbo Wang(王建波), and Qingfang Liu(刘青芳)
Chin. Phys. B, 2022, 31 (**11**): 117505. DOI: 10.1088/1674-1056/ac8af9

Experimental observation of interlayer perpendicular standing spin wave mode with low damping in skyrmion-hosting $[Pt/Co/Ta]_{10}$ multilayer

Zhen-Dong Chen(陈振东), Mei-Yang Ma(马眉扬), Sen-Fu Zhang(张森富), Mang-Yuan Ma(马莽原), Zi-Zhao Pan(潘咨兆), Xi-Xiang Zhang(张西祥), Xue-Zhong Ruan(阮学忠), Yong-Bing Xu(徐永兵), and Fu-Sheng Ma(马付胜)
Chin. Phys. B, 2022, 31 (**11**): 117501. DOI: 10.1088/1674-1056/ac7bf9

Synchronization of nanowire-based spin Hall nano-oscillators

Biao Jiang(姜彪), Wen-Jun Zhang(张文君), Mehran Khan Alam, Shu-Yun Yu(于淑云), Guang-Bing Han(韩广兵), Guo-Lei Liu(刘国磊), Shi-Shen Yan(颜世申), and Shi-Shou Kang(康仕寿)
Chin. Phys. B, 2022, 31 (**7**): 077503. DOI: 10.1088/1674-1056/ac560a

Magnon bands in twisted bilayer honeycomb quantum magnets

Xingchuan Zhu(朱兴川), Huaiming Guo(郭怀明), and Shiping Feng(冯世平)
Chin. Phys. B, 2021, 30 (**7**): 077505. DOI: 10.1088/1674-1056/abeee5

RAPID COMMUNICATION

Nonlinear three-magnon scattering in low-damping $La_{0.67}Sr_{0.33}MnO_3$ thin films

Yuelin Zhang(张跃林)[1,2], Lutong Sheng(盛路通)[1], Jilei Chen(陈济雷)[2,3], Jie Wang(王婕)[4], Zengtai Zhu(朱增泰)[5], Rundong Yuan(袁润东)[1], Jingdi Lu(鲁京迪)[6,4], Hanchen Wang(王涵晨)[1], Sijie Hao(郝思洁)[4], Peng Chen(陈鹏)[7], Guoqiang Yu(于国强)[5,7], Xiufeng Han(韩秀峰)[7], and Haiming Yu(于海明)[1,2,†]

[1] *Fert Beijing Institute, MIIT Key Laboratory of Spintronics, School of Integrated Circuit Science and Engineering, Beihang University, Beijing* 100191, *China*

[2] *International Quantum Academy, Shenzhen* 518048, *China*

[3] *Shenzhen Institute for Quantum Science and Engineering, Southern University of Science and Technology, Shenzhen* 518048, *China*

[4] *Department of Physics, Beijing Normal University, Beijing* 100191, *China*

[5] *Songshan Lake Materials Laboratory, Dongguan* 523808, *China*

[6] *Hefei National Research Center for Physical Sciences at the Microscale, University of Science and Technology of China, Hefei* 230026, *China*

[7] *Beijing National Laboratory for Condensed Matter Physics, Institute of Physics, University of Chinese Academy of Sciences, Chinese Academy of Sciences, Beijing* 100190, *China*

(Received 10 July 2023; revised manuscript received 28 July 2023; accepted manuscript online 8 August 2023)

Three-magnon scattering, a nonlinear process in which a high-energy magnon splits into two low-energy magnons with energy and momentum conservation, has been widely studied in the magnonics community. Here, we report experimental observation of nonlinear three-magnon scattering in $La_{0.67}Sr_{0.33}MnO_3$ thin films with low magnetic damping ($\sim 10^{-4}$) by all-electric and angle-resolved spin wave spectroscopy. The reflection spectra of the spin wave resonance with high-power excitation at Damon–Eshbach configuration demonstrate a scattering regime with gradual signal disappearance, where a magnon of Damon–Eshbach mode decays into two magnons of volume mode above the threshold power (-10 dBm) of the injected microwave. The nonlinear scattering is only allowed at low-field regime and the calculated dispersions of dipole-exchange spin wave claim the mechanism of allowed and forbidden three-magnon scattering. The films and heterostructures of $La_{0.67}Sr_{0.33}MnO_3$ have been already demonstrated with rich physical phenomena and great versatility, in this work the nonlinear magnetic dynamics of $La_{0.67}Sr_{0.33}MnO_3$ thin films is revealed, which offer more possibility for applications to oxide magnonics and nonlinear magnonic devices.

Keywords: spin wave resonance, nonlinear scattering, LSMO films, microwave antenna

PACS: 75.30.Ds, 75.78.–n, 76.50.+g **DOI:** 10.1088/1674-1056/acedf8

1. Introduction

Nonlinear effects have attracted much attention in a wide variety of physical systems, such as optical frequency comb,[1] acoustics,[2,3] magnetic dynamics,[4,5] plasmonics[6] and so on. Spin waves are collective excitations of the magnetic order and their quanta are called magnons, which are regarded as the next generation of information carriers for low-power processing in spintronics and magnonics.[7] Nonlinear magnons have been studied in a lot of magnetic systems for many decades,[8] such as whispering gallery magnons in textures,[9] parallel pumping,[10] Bose–Einstein condensation,[11] magnon Kerr effect[12] and nonlinear level attraction[13] in cavity-magnon systems, and the scattering between magnons and phonons, electrons and themselves,[14] which provides rich physics and further potential in technological applications.[15,16]

Three-magnon scattering is one major nonlinear effect, in which a magnon with energy $\hbar\omega_1$ and finite momentum $\boldsymbol{k}_1$ decays into two lower energy levels, and two scattered magnons have lower energies ($\hbar\omega_2$ and $\hbar\omega_3$) and opposite wave vectors ($\boldsymbol{k}_2$ and $\boldsymbol{k}_3$), respectively. The energy and momentum are conserved in this process,[17] satisfying $\omega_1 = \omega_2 + \omega_3$ and $\boldsymbol{k}_1 = \boldsymbol{k}_2 + \boldsymbol{k}_3$, as shown in Fig. 1(a). It has been demonstrated to generate ultrashort microwave pulse,[18] enhance spin current emission[19] and transfer magnon between different magnets[20] for future application. Three-magnon scattering processes are observed in yttrium iron garnet (YIG) films[21] and heterostructure CoFeB/YIG,[20] NiFe/Cu/CoFe spin valve,[22] NiFe magnetic vortex[23] and so on. The emergence of this phenomenon put forward high requirements for the properties of materials, such as magnetic damping and dispersion relations, making this process generally be driven to half frequency ($\omega_2 = \omega_3 = \omega_1/2$) and become allowed only when half frequency exceeds the minimum of the spin-wave band.[24]

The oxide ferromagnetic material $La_{0.67}Sr_{0.33}MnO_3$ (LSMO) has also attracted a lot of attention and demonstrates the multiple functionalities for potential application in spintronics[25–27] and magnonics.[28–30] The current-

†Corresponding author. E-mail: haiming.yu@buaa.edu.cn

© 2023 Chinese Physical Society and IOP Publishing Ltd

controlled propagation of spin waves is demonstrated in stripe domains of LSMO/$LaAlO_3$ films.[31] and the magnon-polarons with long decay length ($\geq$ 1 mm) in $BiFeO_3$/LSMO heterostructures are realized by magnon–phonon coupling.[32,33] The ultra-low Gilbert damping $\sim 10^{-4}$ of LSMO films is reported with orthorhombic $(110)_o$-orientation $NdGaO_3$ (NGO) substrate.[34] Recently, the room-temperature and zero-field magnetic skyrmions are stabilized by strain-driven Dzyaloshinskii–Moriya interaction in LSMO/NGO (110) films and the hybrid nonreciprocities of spin-wave propagation are reported.[35] But its nonlinear magnetic excitations are not yet reported.

Here, we report the experimental observation of nonlinear three-magnon scattering in low-damping LSMO thin films on NGO (110) substrate by the all-electric and angle-resolved spin wave spectroscopy. The three-magnon scattering can be tuned by microwave power, strength and angle of external field, and it is driven only in low-field regime where the dispersion of exchange-dipolar spin waves satisfies that half frequency exceeds the minimum of the spin-wave band.

2. High-quality thin films

LSMO thin films with a thickness of $\sim$ 150 nm have been grown on NGO $(110)_o$ substrates by pulsed laser deposition with a KrF excimer laser (248 nm). The substrates were heated up to 780 °C and films were deposited under 25 Pa oxygen atmosphere with laser energy density of $\sim$ 0.65 J/cm^2 and laser frequency of 5 Hz, then the samples were slowly cooled (5 °C/min) with 1 am oxygen. The pseudo-cubic $(002)_{pc}$ peaks of θ–2θ x-ray diffraction (XRD) show the single-crystal epitaxial growth of LSMO films with in-plane compressive strain on NGO (110) substrate. The topography was characterized by atomic force microscopy (AFM) as shown in Fig. 1(c), which shows a step terrace and good surface roughness ($<$ 1 nm). The magnetic properties of the LSMO thin films were characterized by vibrating sample magnetometer (VSM) and ferromagnetic resonance (FMR). The in-plane magnetic hysteresis loop shows a saturated field of $\sim$ 40 mT along $[010]_{pc}$ orientation as shown in Fig. 1(d). The FMR power absorption spectra were measured with fixed excitation frequencies and sweeping external magnetic field as shown in Fig. 1(f). The linewidths ΔH were fitted by the Lorentzian function and the damping parameter of the LSMO thin films is estimated by the following equation:[36]

$$\frac{|\gamma|}{2\pi}\mu_0\Delta H = \delta f - 2\alpha f, \tag{1}$$

where $|\gamma|/2\pi = 27.2$ GHz/T is the gyromagnetic ratio, which is estimated from the FMR experimental results. ΔH is the line broadening due to extrinsic mechanisms and film inhomogeneities and α is the intrinsic damping parameter. The damping of $\alpha \sim 9 \times 10^{-4}$ is estimated by the linear fitting of experimental data as shown in Fig. 1(e), which is consistent with previous reports.[34] The structural and magnetic characterizations reveal the high quality of the LSMO thin films.

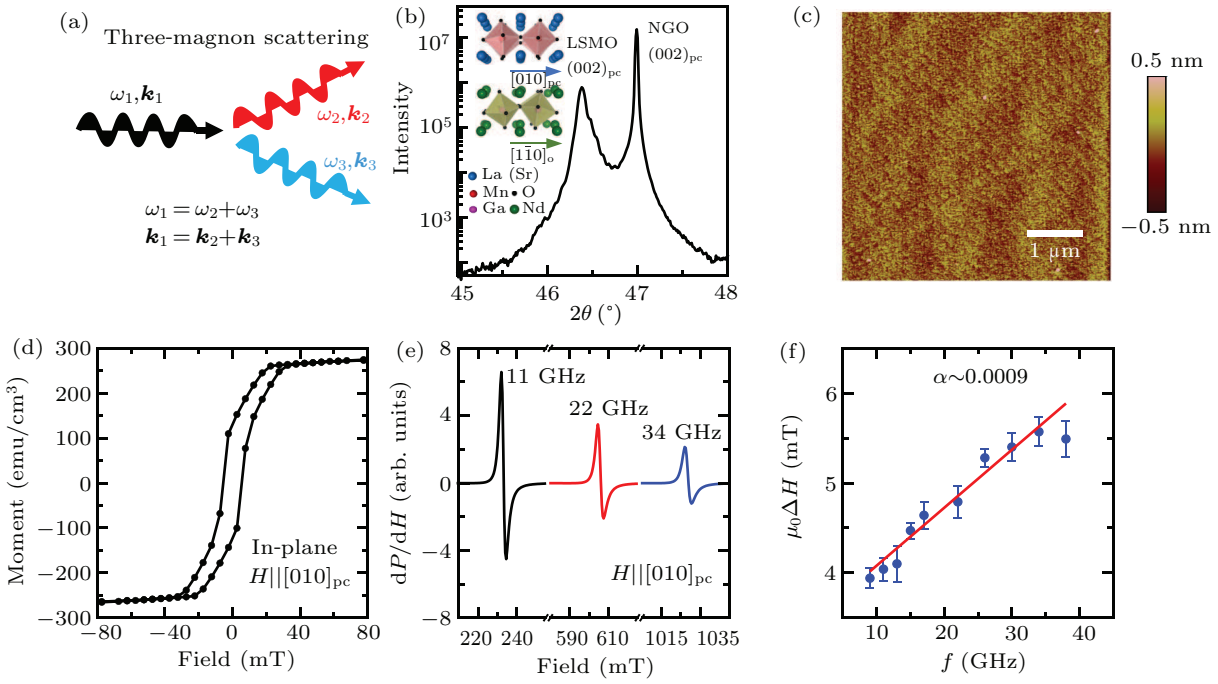


Fig. 1. (a) Schematic of three-magnon scattering with energy and momentum conservation. (b) The x-ray diffraction of LSMO/NGO (110) thin films and schematic of epitaxial relation. The subscript pc and o represent pseudo-cubic and orthorhombic phase. (c) The surface topography of LSMO/NGO (110) thin films captured by atomic force microscopy. The color scale represents surface roughness. (d) The in-plane magnetic hysteresis loop of LSMO/NGO (110) thin films and the external magnetic field is along pseudo-cubic [010] orientation. (e) Ferromagnetic resonance lineplots measured with fixed frequencies under different in-plane applied fields. (f) Ferromagnetic resonance linewidth ΔH as a function of resonance frequency f. Error bars indicate the uncertainty of the linewidth extraction from FMR spectra.

3. Experimental results

3.1. Driving nonlinear scattering

The LSMO thin films were fabricated to hundred-micron sized parallelogram waveguides by laser writing lithography and ion beam etching. Then the patterns of integrated coplanar waveguide (CPW) antennas were fabricated by e-beam lithography and Ti (5 nm)/Au (90 nm) stacks were deposited by magnetron sputtering on top of LSMO waveguides, the signal and ground line widths and edge-to-edge separation are all 0.8 μm, which are characterized by AFM (inset of Fig. 2(a)). The alternating magnetic field is $h_{\rm rf}$ generated by the injected microwave from a vector network analyzer (VNA) and the wavevector k of the excited spin wave is perpendicular to the CPW and along $[100]_{\rm pc}$ direction, and θ is the angle between external magnetic field H and k, as shown in Fig. 2(a). The spatial k distribution of the dynamic field can be calculated by the dimensions of CPW and a Fourier transform as shown in Fig. 2(b), which contains the main excitation at k_1 (~ 1.9 rad/μm) and high-order k_2 (~ 5.5 rad/μm).

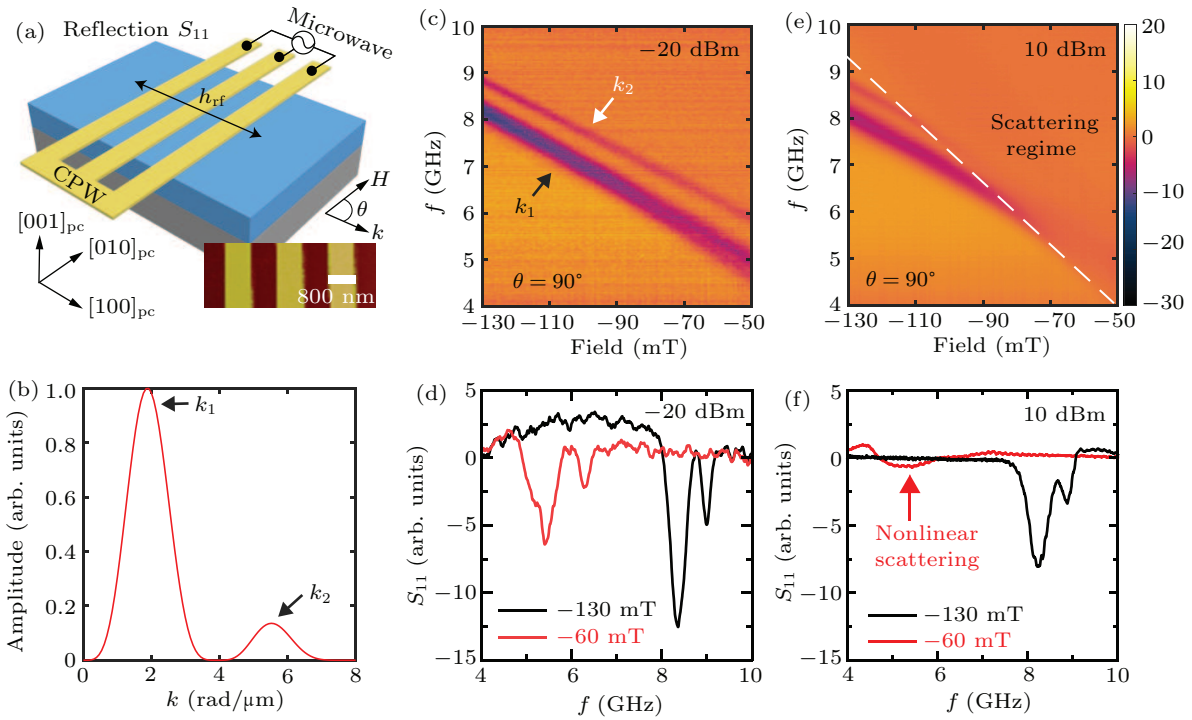


Fig. 2. (a) Sketch of reflection spectra S_{11} measurement, the integrated CPW antenna is fabricated on the top of LSMO/NGO thin films. The inset is the AFM image of CPW. (b) The wavevector k excitation profile of the CPW antenna calculated by Fourier transformation. The amplitude is normalized to that of the k_1 excitation. (c) Field-dependent reflection spectra with low microwave power of −20 dBm and k perpendicular to H. (d) The lineplots of single reflection spectrum taken from (c) at −60 mT and −130 mT. (e) Field-dependent reflection spectra with high microwave power of 10 dBm and k perpendicular to H, the scattering regime is separated by dashed white line. (f) The lineplots of single reflection spectrum taken from (e) at −60 mT and −130 mT.

The field-dependent reflection spectra S_{11} of spin wave resonance are measured by VNA at $\theta = 90°$ configuration when magnetization M is saturated. The magnetostatic surface waves (MSSWs), also known as Damon–Eshbach (DE) modes, are excited with k being perpendicular to the magnetization M. The two branches, which vary characteristically with H, are observed under low excitation with microwave power of −20 dBm (0.01 mW), as shown by color-coded spectra in Fig. 2(c), and lower and higher branches of DE modes are corresponding to the k_1 and k_2 excitations, respectively. The two lineplots of single spectrum extracted at −60 mT and −130 mT are shown in Fig. 2(d) and resonance peaks are clearly visible. The spectra under high excitation with microwave power of 10 dBm (10 mW) are shown in Fig. 2(e) and the image is separated by a dotted white line for eye guidance. The resonance signals are almost gone due to nonlinear scattering around the low-field regime, which is called scattering regime to the right of the dotted line. When the single spectrum under high excitation is extracted at −60 mT as shown in Fig. 2(f), the significant differences can be observed comparing the high excitation at −130 mT or the low excitation at −60 mT. So, this nonlinear scattering can be tuned by the strength of the external magnetic field.

3.2. Mechanism of three-magnon scattering

To clarify the mechanism of nonlinear scattering, the angle-dependent spin wave spectra are measured. Figure 3(a) shows the spectra measured at −60 mT with low excitation of −20 dBm, with the transition from $\theta = 90°$ to $\theta = 0°$, the backward volume magnetostatic waves (BVMSWs) are excited with k being parallel to the magnetization M, which is called BV modes simplistically. The spectra of spin wave resonance depend strongly on the angle θ due to the contribution of dipole–dipole interaction when the thin film is in-plane

magnetized. The dipole–dipole interaction will be dominant in the regime with small k and the isotropic exchange interaction begins to be dominant in the regime with large k. The dipole–dipole contribution to the dispersion relation leads to a negative group velocity of the BV modes and a positive group velocity of the DE modes, this is the reason that the high-order mode is excited with lower frequency at BV ($\theta = 0°$) configuration, which is opposite to DE ($\theta = 90°$) configuration.

When the microwave power is increased to 10 dBm as shown in Fig. 3(b), the BV spin wave resonance modes are still clearly visible but the DE spin wave resonance modes are almost gone, which means that the nonlinear scattering is mainly driven for MSSWs around $\theta = 90°$. So, this nonlinear scattering can be tuned by the angle of external magnetic field. The color scales of the two spectra are unified but they have different noise levels due to the large difference of the injected microwave power.

So, the dispersions of DE and BV modes are calculated to further clarify the physical mechanism. Considering the ~ 150 nm thickness of the LSMO film and finite k excitation over ~ 1 rad/μm, the dispersion equation of dipole-exchange spin waves derived by Kalinikos and Slavin[37,38] is used as follows:

$$f_{\mathrm{DE}} = \frac{|\gamma|\mu_0}{2\pi}\left[\left(H+\frac{2A}{\mu_0 M_\mathrm{s}}k^2\right)\times\left(H+\frac{2A}{\mu_0 M_\mathrm{s}}k^2+M_\mathrm{s}\right)+M_\mathrm{s}^2\left(\frac{1-\mathrm{e}^{-2kt}}{4}\right)\right]^{\frac{1}{2}}, \tag{2}$$

$$f_{\mathrm{BV}} = \frac{|\gamma|\mu_0}{2\pi}\left[\left(H+\frac{2A}{\mu_0 M_\mathrm{s}}k^2\right)\times\left(H+\frac{2A}{\mu_0 M_\mathrm{s}}k^2+M_\mathrm{s}\frac{1-\mathrm{e}^{-kt}}{kt}\right)\right]^{\frac{1}{2}}, \tag{3}$$

where $A = 1.92$ J/m is the exchange constant,[39] $M_\mathrm{s} = 260$ emu/cc is the saturated magnetization extracted from VSM, and $t = 150$ nm is the thickness of the LSMO thin film.

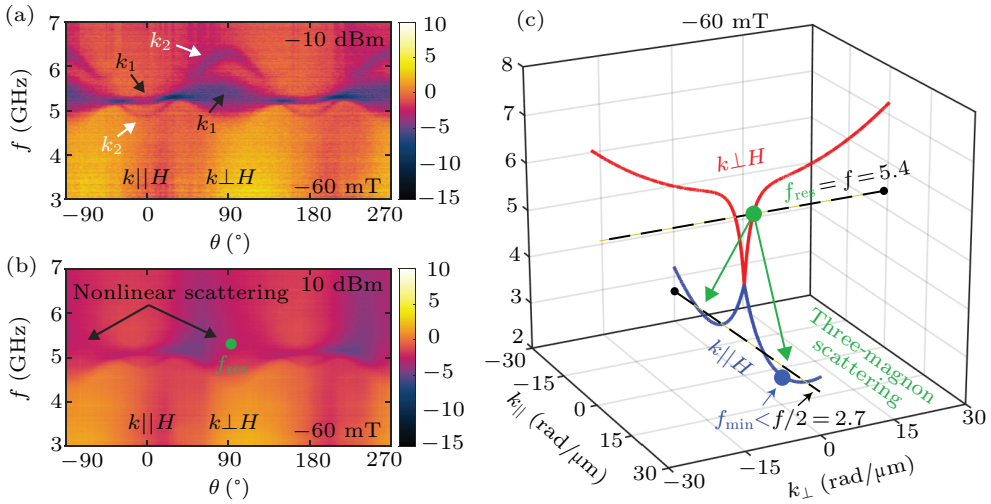


Fig. 3. (a) The angle-dependent reflection spectra with low microwave power of −10 dBm and external field of −60 mT, where nonlinear scattering is not driven. (b) The angle-dependent reflection spectra with high microwave power of 10 dBm and external field of −60 mT, where nonlinear scattering is mainly driven around $k \perp H$. (c) The calculated dispersion of ∼ 150 nm LSMO/NGO thin films at −60 mT. The green dots in (b) and (c) represent resonance frequency excited with k_1 in experiments. The blue dot represents the minimum energy position of magnon at $k \parallel H$ configuration. The green arrows represent that three-magnon scattering is allowed from frequency f to half-frequency $f/2$, which are marked by two dashed black lines.

The calculated dispersions at −60 mT are shown in Fig. 3(c), the red and blue lines are the dispersion of dipole-exchange spin waves at DE and BV configurations, respectively. The resonance frequency of operating point at DE mode with k_1 is $f \sim 5.4$ GHz, which is marked by green dots (f_{res}) both in experimental result and calculation of Figs. 3(b) and 3(c). The dashed black lines represent the positions of frequency f and half-frequency $f/2$. The minimum energy position of BV mode is ~ 2.57 GHz, which is lower than half-frequency $f/2 \sim 2.7$ GHz, which means that the magnon scattering from frequency f to half-frequency $f/2$ is allowed in this configuration. One nonlinear magnon with f at DE mode splits into two parametric magnons with $f/2$ and opposite k, which satisfy energy and momentum conservation under three magnon splitting. The wavevectors of half-frequency magnons are as high as ±15 rad/μm and the wavelength is about 420 nm.

Then, the power-dependent spin wave spectra are measured at both −60 mT and −130 mT. As shown in Fig. 4(a), the nonlinear effect is gradually driven with the increasing microwave power and scattering can be observed clearly over about −10 dBm. But the same experimental phenomenon is not observed at −130 mT as shown in Fig. 4(b), there is still negative nonlinear frequency shift with high excitation, which means that the magnons go into the nonlinear regime. With the increase of the external field from −60 mT to −130 mT, the resonance frequency of operating point at DE mode with k_1 is

$f \sim 8.1$ GHz, which is also marked by green dots ($f_{\rm res}$) both in experimental result and calculation of Figs. 4(b) and 4(c). The dispersions of dipole-exchange spin waves at -130 mT are shown in Fig. 4(c), the minimum energy position of BV mode is ~ 4.68 GHz, which is larger than the half-frequency $f/2 \sim 4.05$ GHz and means that the magnon scattering from frequency f to half-frequency $f/2$ is not allowed in this configuration.

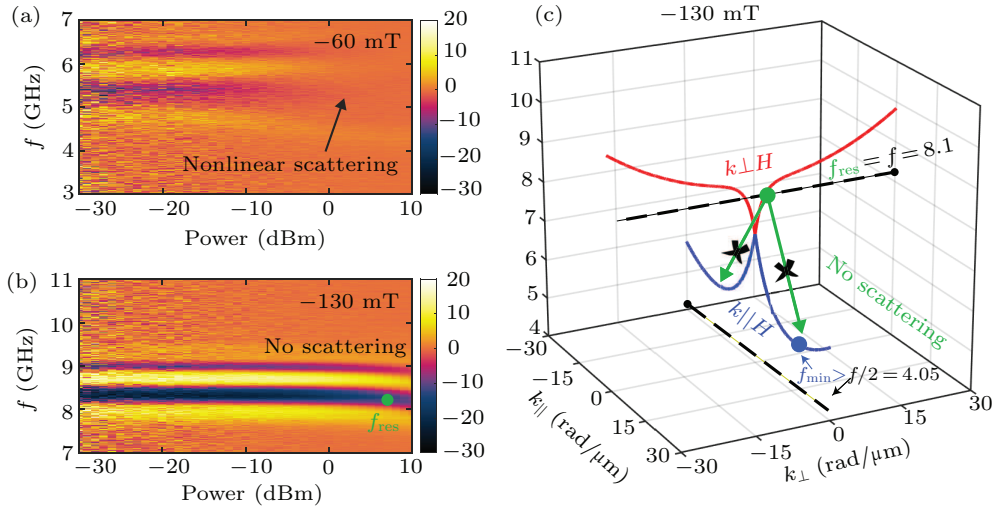


Fig. 4. (a) The power-dependent reflection spectra at -60 mT, where nonlinear scattering is driven over threshold of -10 dBm. (b) The power -dependent reflection spectra at -130 mT, where nonlinear scattering is not driven even with 10 dBm. (c) The calculated dispersion of ~ 150 nm LSMO/NGO thin films at -130 mT. The green dots in (b) and (c) represent resonance frequency excited with k_1 in experiments. The blue dot represents the minimum energy position of magnon at $k \parallel H$ configuration. The green arrows with black cross represent that three-magnon scattering is not allowed from frequency f to half-frequency $f/2$, which are marked by two dashed black lines.

4. Conclusion and perspectives

In conclusion, the nonlinear three-magnon scattering of LSMO films with low magnetic damping is excited and detected by nanoscale CPW antennas and VNA. The scattered magnons are driven with microwave power over -10 dBm, and one DE magnon splits into a pair of volume mode magnons with opposite wavevectors. This nonlinear splitting process can be also tuned by the strength and angle of the in-plane external field. The calculated dispersion of dipole-exchange spin waves claims that the three-magnon scattering will be only allowed at the low-field regime, where the minimum energy level of BV mode is lower than the half-frequency of the resonant magnon. The nonlinearity in magnetization dynamics of LSMO films demonstrates its application potential in functional oxide magnonics and provides one more material platform for nonlinear magnonics.[40] Considering the advantage of strained LSMO films in magnetic textures and electric reconfigurability, the experimental implementation of nonlinearity in nontrivial magnetic spirals and skyrmions[41–43] and current-controlled scattering process[22] in LSMO films are promising in future.

Acknowledgements

Project supported by the National Key Research and Development Program of China (Grant No. 2022YFA1402801). Yuelin Zhang thanks the support from the China Postdoctoral Science Foundation Funded Project (Grant No. 2021M700344). Project supported also by the National Natural Science Foundation of China (Grant Nos. 12074026, 12104208, and U1801661). Lutong Sheng thanks the support from the Academic Excellence Foundation of BUAA for PhD Students.

References

[1] Udem T, Holzwarth R and Hänsch T W 2002 *Nature* **416** 233
[2] Ostrovsky L A 1999 *J. Acoust. Soc. Am.* **105** 578
[3] Shao L, Mao W, Maity S, Sinclair N, Hu Y, Yang L and Lončar M 2020 *Nat. Electron.* **3** 267
[4] Wu W J, Xu D, Qian J, Li J, Wang Y P and You J Q 2022 *Chin. Phys. B* **31** 127503
[5] Lévov V 1994 *Wave turbulence under parametric excitations: applications to magnetics* (Berlin: Springer)
[6] Kauranen M and Zayats A V 2012 *Nat. Photon.* **6** 737
[7] Han X F, Wan C H, Wu H, Guo C Y, Tang P, Yan Z R, Xing Y W, He W Q and Yu G Q 2022 *Chin. Phys. B* **31** 117504
[8] Demokritov S 2001 *Phys. Rep.* **348** 441
[9] Schultheiss K, Verba R, Wehrmann F, Wagner K, Korber L, Hula T, Hache T, Kakay A, Awad A A, Tiberkevich V, Slavin A N, Fassbender J and Schultheiss H 2019 *Phys. Rev. Lett.* **122** 097202
[10] Brächer T, Pirro P and Hillebrands B 2017 *Phys. Rep.* **699** 1
[11] Schneider M, Bracher T, Breitbach D, Lauer V, Pirro P, Bozhko D A, Musiienko-Shmarova H Y, Heinz B, Wang Q, Meyer T, Heussner F, Keller S, Papaioannou E T, Lagel B, Lober T, Dubs C, Slavin A N, Tiberkevich V S, Serga A A, Hillebrands B and Chumak A V 2020 *Nat. Nanotechnol.* **15** 457
[12] Wang Y P, Zhang G Q, Zhang D, Luo X Q, Xiong W, Wang S P, Li T F, Hu C M and You J Q 2016 *Phys. Rev. B* **94** 224410
[13] Xiao Y, Wang H, Wang D, Lu R, Yan X, Guo H, Hu C M, Xia K, Zhang H and Xing D 2021 *Phys. Rev. B* **104** 115147
[14] Gurevich A G and Melkov G A 1996 *Magnetization oscillations and waves* (CRC press)
[15] Slavin A and Tiberkevich V 2009 *IEEE Trans. Magn.* **45** 1875
[16] Ustinov A B, Drozdovskii A V and Kalinikos B A 2010 *Appl. Phys. Lett.* **96** 142513
[17] Pirro P, Vasyuchka V I, Serga A A and Hillebrands B 2021 *Nat. Rev. Mater.*

[18] Synogach V T, Fetisov Y K, Mathieu C and Patton C E 2000 *Phys. Rev. Lett.* **85** 2184
[19] Kurebayashi H, Dzyapko O, Demidov V E, Fang D, Ferguson A J and Demokritov S O 2011 *Nat. Mater.* **10** 660
[20] Sheng L, Elyasi M, Chen J, He W, Wang Y, Wang H, Feng H, Zhang Y, Medlej I, Liu S, Jiang W, Han X, Yu D, Ansermet J P, Bauer G E W and Yu H 2023 *Phys. Rev. Lett.* **130** 046701
[21] Mathieu C, Synogatch V T and Patton C E 2003 *Phys. Rev. B* **67** 104402
[22] Schultheiss H, Janssens X, van Kampen M, Ciubotaru F, Hermsdoerfer S J, Obry B, Laraoui A, Serga A A, Lagae L, Slavin A N, Leven B and Hillebrands B 2009 *Phys. Rev. Lett.* **103** 157202
[23] Korber L, Schultheiss K, Hula T, Verba R, Fassbender J, Kakay A and Schultheiss H 2020 *Phys. Rev. Lett.* **125** 207203
[24] Bertelli I, Simon B G, Yu T, Aarts J, Bauer G E W, Blanter Y M and Sar T 2021 *Adv. Quantum Technol.* **4** 2100094
[25] Liao Z, Huijben M, Zhong Z, Gauquelin N, Macke S, Green R J, Van Aert S, Verbeeck J, Van Tendeloo G, Held K, Sawatzky G A, Koster G and Rijnders G 2016 *Nat. Mater.* **15** 425
[26] Yi D, Liu J, Hsu S L, Zhang L, Choi Y, Kim J W, Chen Z, Clarkson J D, Serrao C R, Arenholz E, Ryan P J, Xu H, Birgeneau R J and Ramesh R 2016 *Proc. Natl. Acad. Sci. USA* **113** 6397
[27] Zhang H, Zhang J, Zhang J E, Han F R, Huang H L, Song J H, Shen B G and Sun J R 2019 *Chin. Phys. B* **28** 037501
[28] Wahler M, Homonnay N, Richter T, Muller A, Eisenschmidt C, Fuhrmann B and Schmidt G 2016 *Sci. Rep.* **6** 28727
[29] Luo G Y, Lin J G, Chiang W C and Chang C R 2017 *Sci. Rep.* **7** 6612
[30] Zhang Y, Chen J, Zhang J and Yu H 2022 *Appl. Phys. Rev.* **9** 041312
[31] Liu C, Wu S, Zhang J, Chen J, Ding J, Ma J, Zhang Y, Sun Y, Tu S, Wang H, Liu P, Li C, Jiang Y, Gao P, Yu D, Xiao J, Duine R, Wu M, Nan C W, Zhang J and Yu H 2019 *Nat. Nanotechnol.* **14** 691
[32] Zhang J, Chen M, Chen J, Yamamoto K, Wang H, Hamdi M, Sun Y, Wagner K, He W, Zhang Y, Ma J, Gao P, Han X, Yu D, Maletinsky P, Ansermet J P, Maekawa S, Grundler D, Nan C W and Yu H 2021 *Nat. Commun.* **12** 7258
[33] Chen J, Yamamoto K, Zhang J, Ma J, Wang H, Sun Y, Chen M, Ma J, Liu S, Gao P, Yu D, Ansermet J P, Nan C W, Maekawa S and Yu H 2023 *Phys. Rev. Appl.* **19** 024046
[34] Qin Q, He S, Song W, Yang P, Wu Q, Feng Y P and Chen J 2017 *Appl. Phys. Lett.* **110** 112401
[35] Zhang Y, Liu J, Dong Y, Wu S, Zhang J, Wang J, Lu J, Rückriegel A, Wang H, Duine R, Yu H, Luo Z, Shen K and Zhang J 2021 *Phys. Rev. Lett.* **127** 117204
[36] Kuanr B, Camley R E and Celinski Z 2005 *Appl. Phys. Lett.* **87** 012502
[37] Kalinikos B A and Slavin A N 1986 *J. Phys. C: Solid State Phys.* **19** 7013
[38] Wang H, He W, Yuan R, Wang Y, Wang J, Zhang Y, Medlej I, Chen J, Yu G, Han X, Ansermet J-P and Yu H 2022 *Phys. Rev. B* **106** 064410
[39] Wang J, Xie L S, Wang C S, Zhang H Z, Shu L, Bai J, Chai Y S, Zhao X, Nie J C, Cao C B, Gu C Z, Xiong C M, Sun Y, Shi J, Salahuddin S, Xia K, Nan C W and Zhang J X 2014 *Phys. Rev. B* **90** 224407
[40] Prabhakar A and Stancil D D 2009 *Spin waves: Theory and applications*, Vol. 5 (Springer)
[41] Wang Z, Yuan H Y, Cao Y, Li Z X, Duine R A and Yan P 2021 *Phys. Rev. Lett.* **127** 037202
[42] Zhou Z W, Wang X G, Nie Y Z, Xia Q L and Guo G H 2021 *J. Magn. Magn. Mater.* **534** 168046
[43] Zhang B, Wang Z, Cao Y, Yan P and Wang X R 2018 *Phys. Rev. B* **97** 094421